

Vapor–Liquid Equilibrium and Critical Line of the CO₂ + Xe System. Critical Behavior of CO₂ + Xe versus CO₂ + *n*-Alkanes

Nuno Ribeiro,* Teresa Casimiro, Catarina Duarte, Manuel Nunes da Ponte, and Ana Aguiar-Ricardo*,‡

Departamento de Química, Centro de Química Fina e Biotecnologia, Faculdade de Ciências e Tecnologia, Universidade Nova de Lisboa, 2825-114 Caparica, Portugal

Martyn Poliakoff

The School of Chemistry, University of Nottingham, Nottingham NG7 2RD, England

Received: June 14, 1999; In Final Form: November 24, 1999

An acoustic technique was applied to investigate the binary critical behavior of the system CO₂ + Xe. The critical line of this binary system exhibits a temperature minimum, suggesting the existence of azeotropic behavior. The compositions of the studied mixtures were chosen in order to define the minimum temperature locus ($p = 6.04$ MPa, $T = 282.34$ K and at $x(\text{CO}_2) = 0.3622$). The results were correlated with the Peng–Robinson equation of state using conventional mixing and combining rules. Additionally, the same equation was used to correlate published data on CO₂ with the five lower normal alkanes. The adjustable interaction energy and size parameters for CO₂ + Xe are in line with those from CO₂ + C₂H₆ up to CO₂ + C₅H₁₂, while those for CO₂ + CH₄ deviate significantly.

Introduction

Because of its extreme molecular simplicity, xenon has been used as a model component of liquid mixtures used to test fundamental statistical theories of the liquid state. Thermodynamic properties of fluid mixtures containing xenon have been studied by a large number of authors. The 1975 compilation of Hiza, Kidnay and Miller on equilibrium properties of fluids of cryogenic interest,¹ for instance, includes 24 references to publications on binary mixtures containing xenon. Since then, experimental data on Xe containing mixtures have continued to be published. In particular, results on mixtures of xenon with the lower hydrocarbons have proved to be particularly interesting for theory testing and development.^{2–12}

The carbon dioxide molecule is small and compact, with a strong quadrupole,¹³ which makes it also a relevant testing ground for theory. Apart from this interest for theory testing, CO₂ has also been much studied recently, due to its possible applications as an alternative “green” solvent in extraction, reaction, and particle formation processes in supercritical media.^{14,15} In particular, the effect on reactivity of a solvent with a tunable density, such as a supercritical fluid, has recently attracted much attention.¹⁶

Mixtures of carbon dioxide and xenon could provide an ideal medium to carry out studies of that tunability effect. Both substances have critical temperatures close to ambient temperatures (16 °C for xenon, 31 °C for CO₂) and accessible critical pressures (5.8 and 7.4 MPa), and therefore they can easily be handled as supercritical gases. More important, their properties as solvents are very different.

Calado and collaborators¹⁷ have studied the thermodynamics of liquid mixtures of xenon with the lower alkanes and with the lower perfluoroalkanes. They found that while xenon +

alkane are highly ideal mixtures, xenon + perfluoroalkane exhibit high positive deviations to ideality. Moreover, application of the statistical associating fluid theory (SAFT)¹⁸ to these mixtures was very successful when the characteristic molecular parameters for Xe, sphere diameter and mean field energy, were the average values of the parameters obtained for the alkanes. On the other hand, Johnston¹⁹ indicates that supercritical carbon dioxide behavior is closer to a perfluoroalkane. In fact, much recent work on polymerization²⁰ in supercritical carbon dioxide has produced, for instance, fluoroacrylate polymers with the same properties as those obtained in chlorofluorocarbons. These and similar results were attributed to specific interactions between carbon dioxide and the polar fluorine containing group.

Liquid mixtures of alkanes and perfluoroalkanes are highly nonideal,^{21,22} indicating strong differences in the molecular interactions established by each mixture component. It is reasonable to assume that supercritical mixtures of carbon dioxide and xenon might provide an environment for reactants and activated complex in a reaction that would be easily tunable not only in terms of density but also in terms of molecular interactions, by changing the composition of the solvent. For this type of study, knowledge of the critical line in the phase diagram is essential, to locate the pressure and temperature working conditions.

The only study of the critical line available until now is the work of Martynets et al.²³ They reported experimental (p, ρ, T, x) data for the critical curve of $\{x\text{Xe} + (1 - x)\text{CO}_2\}$ but restricted to the region near the critical point of pure carbon dioxide, with x between 0 and 4.2067×10^{-2} .

In this paper, we first describe the principle of the acoustic method when applied to mixtures. A new apparatus and the experimental procedure to obtain vapor–liquid equilibrium and critical data are described in detail. The binary mixture CO₂ + Xe was studied over the whole composition range. The results

‡ E-mail: aar@dq.fct.unl.pt. Fax: 351-212948385.

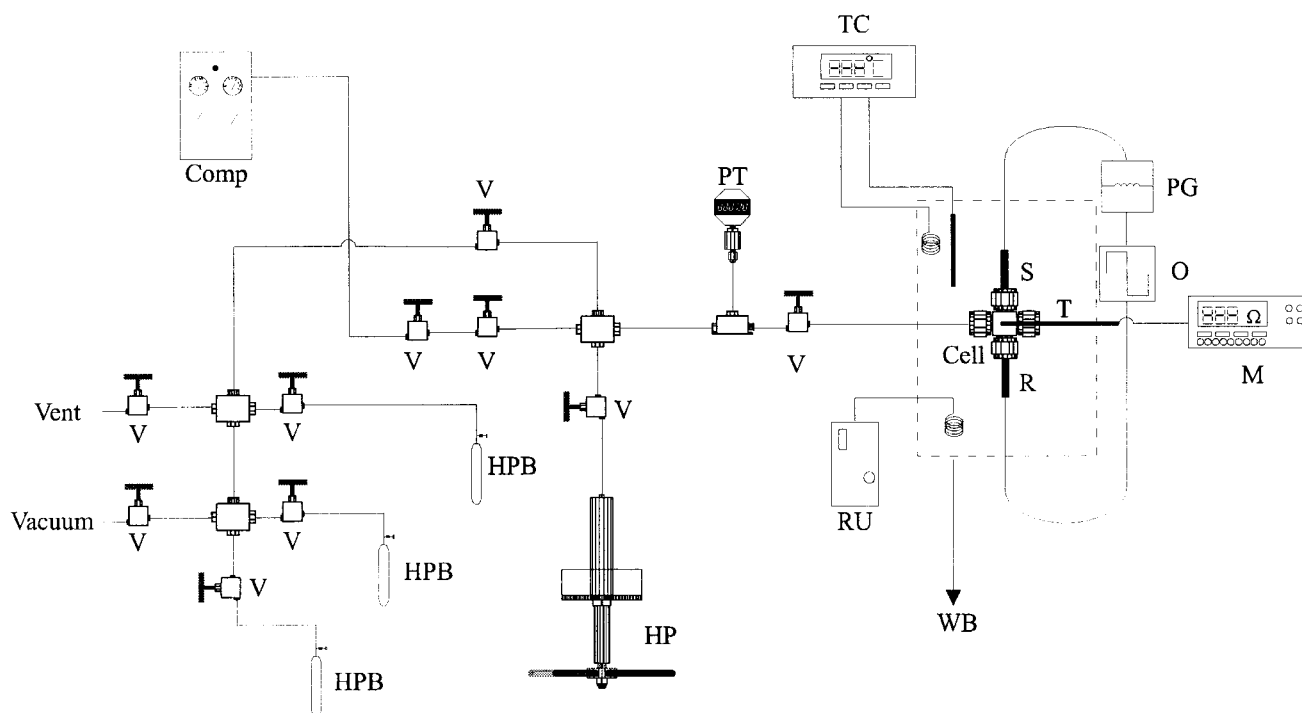


Figure 1. Acoustic apparatus: Comp, compressor; HP, hand pump; HPB, high-pressure bomb; M, multimeter; O, oscilloscope; PG, pulse generator; PT, pressure transducer; RU, refrigeration unit; T, platinum resistance thermometer; V, valves; WB, water bath.

show that this system deviates strongly from ideality. The critical p - T line exhibits a temperature minimum, suggesting the existence of a positive azeotrope.

The Peng-Robinson equation of state (PR EOS),²⁴ with conventional mixing and combining rules, was used to correlate experimental data. Additionally, the same equation was used to correlate previously published data on CO₂ with the five lower n -alkanes, to compare the critical behavior of these systems with CO₂ + Xe. k_{ij} and l_{ij} , the deviation parameters from the geometric and arithmetic mean combining rules for the cross interactions, were calculated and compared for all systems.

Principles of the Method

To apply the acoustic technique to the measurement of critical parameters, we must explore the isothermal compressibility, the physical property that undergoes a sudden change at the critical point. The isothermal compressibility ($k_T = -1/V(\partial V/\partial p)_T$) of a pure substance diverges to infinity in the immediate vicinity of the critical point.²¹ This is accompanied by a corresponding decrease in the velocity and increased attenuation of sound waves through the medium.

For mixtures, the conditions for the compressibility divergence at a critical point are met only when an azeotrope persists up to the critical line. In other cases, the compressibility is finite. However, if the critical point is approached from the one-phase region, the compressibility may be seen to increase up to the critical point as pointed out by Levelt Sengers.²⁵

Experimental Apparatus

Using this property, Kordikowski et al.^{26,27} and Aguiar-Ricardo et al.²⁸ obtained critical temperatures and pressures in close agreement with previously published results obtained by other methods,²⁹⁻³² such as direct visual inspection of the critical opalescence, or by sampling. The critical parameters were obtained by measuring the transit time of the ultrasonic pulse

between two piezoelectric transducers through a thermostated fluid mixture, as a function of pressure.

The acoustic apparatus used in this work is similar to the one described by Kordikowski et al.²⁶ and is schematically represented in Figure 1. The acoustic cell is constructed from a stainless steel $3/8$ in. cross piece, with its inner diameter bored out to provide an acoustic cavity of about 5 mL volume. Pressure was generated via a hand pump (High-Pressure Equipment Co., model 62-6-10) and monitored with a pressure transducer (Omega, model PX931) with a precision of ± 0.01 MPa. Temperature was measured on the ITS-90 with a precision of ± 0.001 K with a calibrated platinum resistance thermometer (Tinsley) connected to a digital multimeter (Keithley, model 2000). A pulse generator (Wavetek, model 80) provided the acoustic signal, with a frequency of about 300 kHz. The signal was fed into the acoustic cavity via a piezoelectric ceramic transducer (Morgan Matroc Ltd., PC4D). A second, identical transducer monitored the signal at the other end of the cavity. The transit times of the pulse across the acoustic cavity were displayed in an oscilloscope (Tektronix, model TDS-340). The acoustic cell was immersed in a 40 L water bath, thermostated with a refrigeration unit and a temperature controller from Hart Scientific, with a RTD probe. This unit provides a temperature control within ± 0.004 K.

A mixture with a desired composition was obtained by weighing and was pumped into the acoustic cell. The pressure was increased with the hand pump until only minute changes in the acoustic signal were observed, meaning that a liquid like state with a low compressibility was present in the acoustic cell. The system was allowed to equilibrate for at least 30 min at the desired starting temperature to guarantee that a homogeneous liquid phase was present. Experiments were carried out at constant temperature and pressure was lowered until a maximum in time delay was observed. The temperature was then systematically varied and the procedure repeated. The temperature and pressure values corresponding to the absolute maximum of time delay in the ensemble of the isothermal curves ($t_{\text{delay}}/\mu\text{s}$ vs

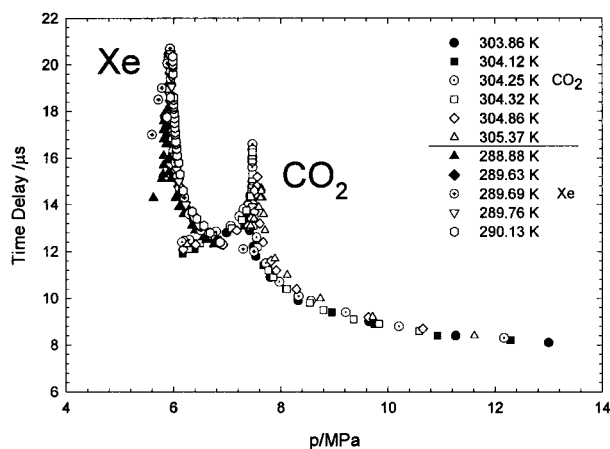


Figure 2. Acoustic data for pure Xe and CO₂. Full symbols represent subcritical isotherms. Open symbols represent supercritical isotherms. The critical isotherm is represented with a center-dotted circle.

TABLE 1: Critical Temperature, T_c , and Critical Pressure, p_c , of the Pure Components, Xe and CO₂ (Comparison between Experimental and Literature Values^{33,34})

	p_c/MPa	$p_c - p_c(\text{lit.})/\text{MPa}$	T_c/K	$T_c - T_c(\text{lit.})/\text{K}$
Xe	5.88 ± 0.05	0.04^{33}	289.69 ± 0.05	-0.01^{33}
CO ₂	7.42 ± 0.05	0.04^{34}	304.25 ± 0.05	0.05^{34}

TABLE 2: Experimental Critical Data, p_c and T_c , of the Binary System CO₂ + Xe

x_{CO_2}	p_c/MPa	T_c/K
0.90	7.15	298.47
0.75	6.78	291.33
0.51	6.20	283.31
0.36	6.04	282.34
0.25	6.01	283.84
0.09	5.91	286.88

p/MPa) were taken as the critical temperature and pressure. Figure 2 explains this procedure for the pure components.

CO₂ and Xe were supplied by Air Liquide with purities higher than 99.99 mol %. Both gases were used without further purification.

Results and Discussion

Pure Components. To further evaluate the feasibility of the method and the accuracy of the apparatus, experimental critical data on CO₂ and Xe were obtained and compared with published values.^{33,34} Several isotherms were measured in the vicinity of the critical temperature, and experimental data are plotted in Figure 2, as a time delay–pressure diagram. Table 1 shows that the critical temperature and pressure of the pure components measured in our apparatus are in agreement with the literature values within the combined experimental errors.

Binary Mixtures. To investigate the critical behavior of the CO₂ + Xe system, acoustic measurements were performed on six mixtures covering the whole mole fraction range. The binary critical data are presented in Table 2 and plotted in Figure 3.

The critical line has a temperature minimum, located at 6.04 MPa, 282.34 K, and at $x(\text{CO}_2) = 0.3622$. Generally, a minimum in the mixture critical temperature is associated with the occurrence of azeotropic behavior.^{21,35,36} There are, however, exceptions, as in the hydrogen sulfide + ethane system,³⁷ where an azeotrope occurs without the existence of temperature extrema, or as in the hydrogen sulfide + isobutane system,³⁸ which has a minimum in the critical temperature but does not present azeotropic behavior.

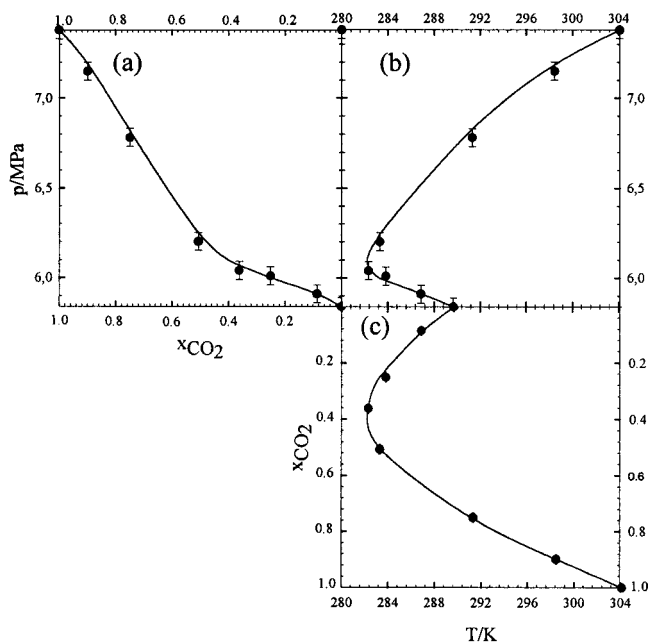


Figure 3. Projections of the binary critical curve of the system CO₂ + Xe: (a) p – x projection; (b) p – T projection; (c) x – T projection; (●) this work; (—) fitted curve to experimental data.

In this case, the minimum in mixture critical temperature and, additionally, the shape of the critical line of CO₂ + Xe system suggest the existence of positive azeotropy (a minimum boiling azeotrope), as in the CO₂ + C₂H₆ system.³⁹

Correlation of Results

Experimental critical data were correlated with the Peng–Robinson equation of state (PR EOS).²⁴

$$p = \frac{RT}{(V-b)} - \frac{a(t)}{V(V+b) + b(V-b)} \quad (1)$$

This equation is the most widely used equation of state in industry, especially for refinery and for process design.⁴⁰ The advantages of the PR EOS are that it requires little input information (critical temperature and pressure and the acentric factor) and little computer time.

The PR EOS was used with the so-called van der Waals one-fluid mixing rules:

$$a_{\text{mix}} = \sum_i \sum_j x_i x_j a_{ij} \quad (2)$$

$$b_{\text{mix}} = \sum_i \sum_j x_i x_j b_{ij} \quad (3)$$

where the a and b for the cross interaction were

$$a_{ij} = (a_i a_j)^{1/2} (1 - k_{ij}) \quad (4)$$

$$b_{ij} = 1/2 [(b_i + b_j)(1 - l_{ij})] \quad (5)$$

x_i is the mole fraction of component i and k_{ij} and l_{ij} are deviation parameters from the geometric and arithmetic mean combining rules for the cross i – j interaction. a_{ii} and b_{jj} are pure component parameters as defined by Peng and Robinson. Values of critical temperature (T_c), critical pressure (p_c), and acentric factor (ω_i) for each pure fluid,³⁴ along with the deviation parameters, constitute the model input variables for PR EOS. The deviation

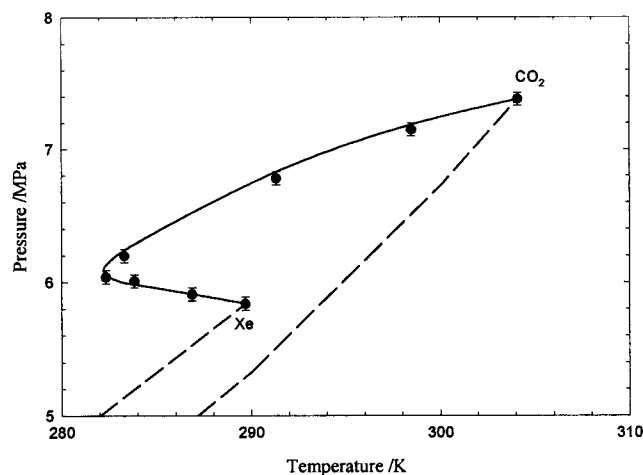


Figure 4. p - T projection of the $\text{CO}_2 + \text{Xe}$ system: (●) this work; (—) predicted critical line with the PR EOS; (---) vapor pressure curves for pure components.⁴¹

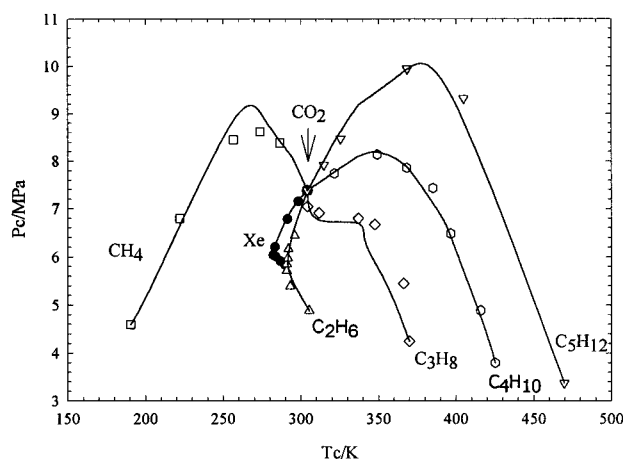


Figure 5. p - T Projection of binary critical lines for the $\text{CO}_2 + \text{Xe}$ and $\text{CO}_2 + n$ -alkanes systems: (●) this work; (□) $\text{CO}_2 + \text{CH}_4$;⁴³ (Δ) $\text{CO}_2 + \text{C}_2\text{H}_6$;⁴² (◇) $\text{CO}_2 + \text{C}_3\text{H}_8$;⁴² (○) $\text{CO}_2 + \text{C}_4\text{H}_{10}$;⁴² (▽) $\text{CO}_2 + \text{C}_5\text{H}_{12}$;⁴² (—) predicted critical line with the PR EOS.

TABLE 3: Deviation Parameters, k_{ij} and l_{ij} , of Each Binary System

binary system	k_{ij}	l_{ij}
$\text{CO}_2 + \text{CH}_4$	0.105	-0.02000
$\text{CO}_2 + \text{Xe}$	0.140	0.00005
$\text{CO}_2 + \text{C}_2\text{H}_6$	0.130	0.00800
$\text{CO}_2 + \text{C}_3\text{H}_8$	0.110	0.0180
$\text{CO}_2 + \text{C}_4\text{H}_{10}$	0.070	0.0200
$\text{CO}_2 + \text{C}_5\text{H}_{12\text{DF}}$	0.040	0.02500

parameters, k_{ij} and l_{ij} , were varied so that the theoretical critical line would give the best fit of the experimental results.

The parameters obtained for $\text{CO}_2 + \text{Xe}$ are included in Table 3, and the p - T projection of the theoretically calculated binary critical line along with the pure component vapor pressures are plotted in Figure 4.

Critical Behavior of $\text{CO}_2 + \text{Xe}$ versus $\text{CO}_2 + n$ -Alkanes

Katz and co-workers^{42,43} reported on the critical behavior of the systems $\text{CO}_2 + \text{CH}_4$, $\text{CO}_2 + \text{C}_2\text{H}_6$, $\text{CO}_2 + \text{C}_3\text{H}_8$, $\text{CO}_2 + \text{C}_4\text{H}_{10}$, and $\text{CO}_2 + \text{C}_5\text{H}_{12}$.

In Figure 5, it can be seen that the shape of the critical loci change sequentially from $\text{CO}_2 + \text{C}_5\text{H}_{12}$ to $\text{CO}_2 + \text{C}_2\text{H}_6$. For instance, the sharp downward curvature of the critical locus at the carbon dioxide end of the curve in the system $\text{CO}_2 + \text{C}_3\text{H}_8$

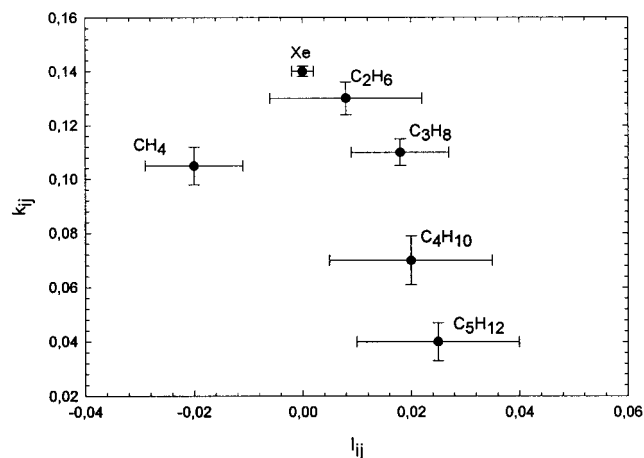


Figure 6. Deviation parameters and error bars for k_{ij} and l_{ij} from the geometric and arithmetic mean combination rules for the cross interaction parameters, a_{ij} and b_{ij} , of each $\text{CO}_2 + \text{X}$ ($\text{X} = \text{CH}_4$, Xe , C_2H_6 , C_3H_8 , C_4H_{10} , C_5H_{12}) binary systems.

is followed by a minimum in the critical temperature and a minimum-boiling azeotrope in $\text{CO}_2 + \text{C}_2\text{H}_6$. It can also be seen that the behavior of $\text{CO}_2 + \text{Xe}$ fits correctly into this sequence, in contrast with the shape of the critical line of $\text{CO}_2 + \text{CH}_4$. These findings seem to be consistent with the above-described work of Calado et al.,¹⁷ where the thermodynamics behavior of liquid xenon in mixtures was shown to be very similar to the behavior of the lower alkanes, except methane.

A correlation of our results and those of Katz and co-workers^{42,43} with the Peng-Robinson equation of state may offer a different insight into our findings.

The PR EOS was used in the same way as described above. The deviation parameters, k_{ij} and l_{ij} , obtained for $\text{CO}_2 +$ lower alkanes are summarized in Table 3. The calculated values of critical parameters of each mixture are displayed as full lines in Figure 5. In this figure, published data and our experimental results are compared with the predicted critical lines. Despite the differences between experimental and calculated values of the critical parameters, a reasonable agreement was obtained and correct composition dependence is observed.

All correlations were performed in this work using the same equation of state, with the same mixing and combining rules, so that the k_{ij} and l_{ij} deviation parameters would be obtained in an internally consistent way. Figure 6 gives a plot of k_{ij} vs l_{ij} . It is well-known that these two parameters are not completely independent of each other; that is, root-mean-square deviations similar to those for the critical parameters can be obtained with different pairs of values. The error bars in Figure 6 were calculated by independently varying either k_{ij} or l_{ij} from the values corresponding to the best fit of experimental critical parameters and given in Table 3. The value of each deviation parameter that would increase the root-mean-square deviation in the critical pressures 5% over its best fit value was taken as the boundary of the error bar. Although this procedure is admittedly arbitrary, it provides a perception of the reliability of the results. Figure 6 shows that the $\text{CO}_2 + \text{Xe}$ deviation parameters can be obtained from a smooth extrapolation of the line running through the corresponding parameters of the $\text{CO}_2 + \text{C}_2\text{H}_6$, $\text{CO}_2 + \text{C}_3\text{H}_8$, $\text{CO}_2 + \text{C}_4\text{H}_{10}$, and $\text{CO}_2 + \text{C}_5\text{H}_{12}$ systems. In contrast, $\text{CO}_2 + \text{CH}_4$ deviates significantly from this line.

Admittedly, this approach is highly empirical and the physical meanings in terms of unlike molecule interaction, of the deviation parameters should be taken cautiously. However, it may at least be said that Figure 6 confirms the findings of Figure

5 and that xenon seems to behave in its mixtures with CO₂ in sequence with the behavior of similar mixtures of the series ethane to *n*-pentane.

Acknowledgment. Financial support from Fundação para a Ciência e Tecnologia, through contracts PBIC/C/QUI/2134/95 and PraxisXXI/BD/16081/98, European Commission, through Contract ERBFMR-CT-97-0104, and Conselho de Reitores das Universidades Portuguesas, through Grant B-39/98, is gratefully acknowledged. M.P. thanks EPSRC, the Royal Academy of Engineering and the Royal Society for support. The authors are grateful to Morgan Matroc Limited for the supply of the piezoelectrics.

References and Notes

- (1) Hiza, M. J.; Kidnay, A. J.; Miller, R. C. *Equilibrium Properties of Fluid Mixtures, A Bibliography of Data on Fluids of Cryogenic Interest*; NSRDS bibliographic Series; IFI/Plenum: New York, 1975.
- (2) Calado, J. G.; Soares, V. A. M. *J. Chem. Thermodyn.* **1977**, *9*, 911.
- (3) Aldersley, S. C.; Lobo, L. Q.; Staveley, L. A. K. *J. Chem. Thermodyn.* **1979**, *11*, 597.
- (4) Calado, J. C. G.; Gomes de Azevedo, E.; Soares, V. A. M. *Chem. Eng. Commun.* **1980**, *5*, 149.
- (5) Lobo, L. Q.; McClure, D. W.; Staveley, L. A. K.; Clancy, P.; Gubbins, K. E.; Gray, C. G. *J. Chem. Soc., Faraday Trans. 2* **1981**, *77*, 425.
- (6) Nunes da Ponte, M.; Chokappa, D.; Calado, J. C. G.; Clancy, P.; Streett, W. B. *J. Phys. Chem.* **1985**, *89*, 2746.
- (7) Bohn, M.; Fischer, J.; Kohler, F. *Fluid Phase Equilib.* **1986**, *31*, 233.
- (8) Nunes da Ponte, M.; Chokappa, D.; Calado, J. C. G.; Zollweg, J.; Streett, W. B. *J. Phys. Chem.* **1986**, *90*, 1147.
- (9) Lainez, A.; Rebelo, L. P. N.; Calado, J. C. G.; Zollweg, J. A. *J. Chem. Thermodyn.* **1987**, *19*, 35.
- (10) Aguiar-Ricardo, A.; Nunes da Ponte, M. *J. Phys. Chem.* **1996**, *100*, 18839.
- (11) Aguiar-Ricardo, A.; Nunes da Ponte, M.; Fischer, J. *J. Phys. Chem.* **1996**, *100*, 18844.
- (12) Duarte, C. M. Ph.D. Thesis, Universidade Nova de Lisboa, Lisbon, 1997.
- (13) Stogryn, D. E.; Stogryn, A. P. *Mol. Phys.* **1966**, *11*, 371.
- (14) Eckert, C. A.; Knutson, B. L.; Debenedetti, P. G. *Nature* **1996**, *383*, 313.
- (15) Darr, J. A.; Poliakoff, M. *Chem. Rev.* **1999**, *99*, 495.
- (16) Kajimoto, O. *Chem. Rev.* **1999**, *99*, 355.
- (17) Filipe, E. J. M.; Dias, L. M. B.; Calado, J. C. G.; McCabe, C. M.; Jackson, G. *Proceedings of the 15th International Conference on Chemical Thermodynamics*; Ribeiro da Silva, M. A. V., Ed.; IUPAC: Porto, 1998.
- (18) Filipe, E. J. M.; Pereira, L. A. M.; Dias, L. M. B.; Calado, J.; Sear, R.; Jackson, G. *J. Phys. Chem. B* **1997**, *101*, 11243.
- (19) Johnston, K. P. *Nature* **1994**, *368*, 187.
- (20) Kendall, J. L.; Canelas, D. A.; Young, J. L.; DeSimone, J. M. *Chem. Rev.* **1999**, *99* (2), 543.
- (21) Rowlinson, J. S.; Swinton, F. L. *Liquids and Liquids Mixtures*, 3rd ed.; Butterworth Scientific: London, 1982.
- (22) Slamoulis, D. Ph.D. Thesis, Delft University of Technology, Delft, 1994.
- (23) Martynets, V. G.; Kuskova, N. V.; Matizen, E. V.; Kukarin, V. F. *J. Chem. Thermodyn.* **1999**, *31*, 191–5.
- (24) Peng, D.; Robinson, D. *Ind. Eng. Chem. Fundam.* **1976**, *15*, 59.
- (25) Levelt Sengers, J. M. H. In *Supercritical Fluids, Fundamentals for Applications*; Kiran, E., Levelt Sengers, J. M. H., Eds.; NATO ASI Ser. E, **273**; Kluwer: Dordrecht, 1994; pp 3–38.
- (26) Kordikowski, A.; Robertson, D. G.; Aguiar-Ricardo, A.; Popov, V. K.; Howdle, S. M.; Poliakoff, M. *J. Phys. Chem.* **1996**, *100*, 9522.
- (27) Kordikowski, A.; Robertson, D. G.; Poliakoff, M.; DiNoia, T. D.; McHugh, M. A.; Aguiar-Ricardo, A. *J. Phys. Chem. B* **1997**, *101*, 5853.
- (28) Aguiar-Ricardo, A.; Ribeiro, N.; Duarte, C. M. M.; Casimiro, T.; Nunes da Ponte, M.; Poliakoff, M. *Proceedings of the 6th Meeting on Supercritical Fluids Chemistry and Materials*; Poliakoff, M., George, M. W., Howdle, S. M., Eds.; International Society for the Advancement of Supercritical Fluids: Nottingham, 1999.
- (29) Moldover, M. R.; Gallagher, J. S. *AIChE J.* **1978**, *24*, 267.
- (30) Weber, L. A. *Int. J. Thermophys.* **1989**, *10*, 617.
- (31) Thorp, N.; Scott, R. L. *J. Phys. Chem.* **1956**, *60*, 670.
- (32) Suehiro, Y.; Nakajima, M.; Yamada, K.; Uematsu, M. *J. Chem. Thermodyn.* **1996**, *28*, 1153.
- (33) Baidakov, V. G.; Rubshtein, A. M.; Pomortsev, V. R.; Sulla, I. J. *Phys. Lett. A* **1988**, *131* (2), 119.
- (34) Angus, S.; Armstrong, B.; de Reuck, K. M. *Carbon Dioxide—International Thermodynamic Tables of the Fluid State-3*; IUPAC, Pergamon Press: Oxford, U.K., 1976.
- (35) Griffiths, R. B.; Wheeler, J. C. *Phys. Rev. A* **1970**, *2* (3), 1047.
- (36) Rainwater, J. C. In *Supercritical Fluid Technology*; Bruno, T. J., Ely, J. F., Eds.; CRC Press: Boca Raton, FL, 1991; pp 129–131.
- (37) Kay, W. B.; Brice, D. B. *Ind. Eng. Chem.* **1953**, *45*, 615.
- (38) Leu, A. D.; Robinson, D. B. *J. Chem. Eng. Data* **1989**, *34*, 315.
- (39) Ohgaki, K.; Katayama, T. *Fluid Phase Equilib.* **1977**, *1*, 27.
- (40) Sandler, S. *Models for Thermodynamic and Phase Equilibria Calculations*, 1st ed.; Marcel Dekker: New York, 1994.
- (41) Reid, R. C.; Prausnitz, J. M.; Pauling, B. E. *The Properties of Gases and Liquids*, 4th ed.; McGraw-Hill: New York, 1987.
- (42) Poettmann, F.; Katz, D. L. *Ind. Eng. Chem.* **1945**, *37*, 9, 847.
- (43) Donnelly, H.; Katz, D. L. *Ind. Eng. Chem.* **1954**, *46*, 3, 511.